

Effect of Nucleotides and Actin on the Orientation of the Light Chain-Binding Domain in Myosin Subfragment 1[†]

Cybelle Smyczynski[‡] and Andrzej A. Kasprzak*

Centre de Recherches de Biochimie Macromoléculaire, CNRS, BP 5051, 34033 Montpellier Cedex, France

Received March 31, 1997; Revised Manuscript Received August 1, 1997[®]

ABSTRACT: The X-ray structure of myosin head (S1) reveals the presence of a long α -helical structure that supports both the essential and the regulatory light chains. It has been proposed that small structural changes in the catalytic domain of S1 are amplified by swinging the long α -helix (the “lever arm”) to produce ~ 11 nm steps. To probe the spatial position of the putative lever in various S1 states, we have measured, by fluorescence resonance energy transfer (FRET), the effect of nucleotides and actin on the distances between Cys-177 of the essential light chain A1 (which is attached to the α -helix) and three loci in the catalytic domain. Cys-177 (donor) was labeled with 1,5-IAEDANS. The trinitrophenylated ADP analog (TNP-ADP, acceptor) was used to measure the distance to the active site. Lys-553 at the actin-binding site, labeled with a fluorescein derivative, and Lys-83 modified with trinitrobenzenesulfonic acid served as two other acceptors. FRET measurements were performed for S1 alone, for its complexes with MgADP and MgATP, for the analogs of the transition state of the ATPase reaction, S1·ADP·BeF_x, S1·ADP·AlF₄, and S1·ADP·VO₄, and for acto–S1 in the absence and in the presence of ADP. When the transition state and acto–S1 complexes were formed, the change in the Cys-177 \rightarrow Lys-83 distance was <1.1 Å, for the distance Cys-177 \rightarrow Lys-553, the change was ± 2.5 Å. These distance changes correspond to rotations by $<10^\circ$ and $\sim 25^\circ$, respectively. For the Cys-177 \rightarrow TNP-ADP the interprobe separation decreased by ~ 6 Å in the presence of BeF_x and AlF₄[–] but only 1.9 Å in the presence of vanadate; we do not interpret the 6 Å change as resulting from the lever rotation. Using the coordinates of the acto–S1 complex, we have computed the expected changes in these distances resulting from rotation of the lever. These changes were much greater than the ones observed. The above results are inconsistent with models of force generation by S1 in which the head assumes two distinct conformations characterized by large differences in the angle between the motor and the light chain-binding domain. Several alternative mechanisms are proposed.

A striking feature of the myosin head, named subfragment 1 or S1,¹ is the presence of two structural domains: a globular motor domain which harnesses the active site as well as the actin-binding site and an 85 Å long helical structure stabilized by two light chains and usually referred to as the light chain-binding domain (I). Models of force generation in muscle have proposed that myosin uses the 85 Å helix as a lever arm to amplify small conformational changes in the catalytic domain that occur as the head cycles through transitory states of the ATPase reaction. To account

for the currently measured step size for myosin, *ca.* 40–110 Å (2–4), a substantial swing of at least 60° is required (5). There exist many lines of experimental evidence supporting the involvement of this helix in the force generation (6–14), although no direct proof of its movement during muscular contraction has so far been presented. There are also some data which do not fit the above model (15). The swinging lever arm hypothesis has recently been extensively reviewed (5, 16–18).

The kinetic intermediate of the myosin chemical reaction in which the structural changes in the head are the most pronounced is believed to be the S1·ADP·P_i state, since upon binding to actin and the release of the phosphate, the myosin head is in the state corresponding to the beginning of the power stroke. S1·ADP·P_i has, however, too short a lifetime to be amenable to standard physicochemical techniques. Therefore, several analogs of the transition state were introduced and commonly used to study this intermediate (19). These are metallofluoride complexes of MgADP: MgADP·BeF_x and MgADP·AlF₄[–] as well as MgADP·VO₄^{3–}. On the basis of high-resolution X-ray structures of the catalytic domain of *Dictyostelium* S1 in these complexes, it was proposed that the beryllium complex of S1 resembles S1·MgATP, whereas the aluminum and the vanadate complexes are analogs of the S1·ADP·P_i state (8, 20). This notion received further support from recent biochemical data (21). These complexes provide an opportunity to freeze the

[†]Funds for this research were provided by the Centre National de la Recherche Scientifique, the Institut National de la Santé et de la Recherche Médicale, and the Association Française contre Myopathies.

* Corresponding author. Phone: +(33) 4 6761-3334. Fax: +(33) 4 6752-1559. E-mail: aak@xerxes.crbm.cnrs-mop.fr.

[‡]In partial fulfillment of her Ph.D. thesis.

[®] Abstract published in *Advance ACS Abstracts*, October 1, 1997.

¹ Abbreviations. DTE, dithioerythritol; EDTA, ethylenediaminetetraacetic acid; FHS, 6-(fluorescein-5- (and 6-) carboxamido)hexanoic acid succinimidyl ester; FRET, fluorescence resonance energy transfer; 1,5-IAEDANS, 5-[[[(2-iodoacetyl)amino]ethyl]amino]naphthalene-1-sulfonic acid; MOPS, 3-(*N*-morpholino)propanesulfonic acid; P_i, orthophosphate, ionization state unspecified; pPDM, *N,N'*-*p*-phenylenedimaleimide; S1, myosin subfragment 1; S1A1 or S1A2, myosin subfragment 1 carrying alkali light chain A1 or A2, respectively; TNBS, 2,4,6-trinitrobenzenesulfonic acid; TNP, trinitrophenyl; TNP-ADP, 2'-(or 3'-) *O*-(2,4,6-trinitrophenyl)adenosine 5'-diphosphate; TNP-ATP, 2'-(or 3'-) *O*-(2,4,6-trinitrophenyl)adenosine 5'-triphosphate; TNP-S1, S1 trinitrophenylated on Lys-83; V_i, orthovanadate, ionization state unspecified.



FIGURE 1: Structure of chicken S1 showing the distances measured in the present work. The coordinates for this graph were obtained from the Brookhaven Protein Data Bank (file name 2MYS). The three tryptic fragments of the S1 heavy chain, 27, 50, and 20 kDa are colored green, red, and blue, respectively. The C-terminal portion of the 20 kDa segment extending from Gly-680 to Lys-884 (the putative lever) is shown in dark blue, whereas the remainder of this fragment is in light blue. The essential light chain (ELC) is shown in yellow and the regulatory light chain (RLC) in magenta.

ATPase cycle of myosin at critical points and to examine the structural properties of the enzyme–product complex at this particular step.

The goal of this paper was to measure by fluorescence resonance energy transfer (FRET) the distances from a chromophore located on the light chain (which is attached to the lever arm) to three chemical points in the motor domain of skeletal muscle S1: Lys-83, the active site, and Lys-553 (Figure 1). The measurements were performed for S1 without nucleotides and for its complexes with ADP, ATP, ADP·BeF_x, ADP·AlF₄[−], ADP·VO₄^{3−}, and actin. Surprisingly, changes in these distances in the presence of the analogs and actin were found to be small. This finding is inconsistent with models of force generation in muscle in which S1 cycles through two distinct conformations characterized by large differences in the angle between the motor and the light chain-binding domain. A preliminary report of these results has been published (22).

EXPERIMENTAL PROCEDURES

Proteins. Actin and the A1 isoform of myosin subfragment 1 (S1A1), both from rabbit skeletal muscle, were prepared as described previously (23). Labeling of Cys-177 of S1A1 was done *in situ* rather than using the commonly employed light chain exchange procedure since there has been a report that modification of the cysteine residue distorts the structure of the light chain (24). In order to avoid the labeling of Cys-707 (SH1), this residue was preblocked with 2,4-dinitro-1-fluorobenzene (Fluka) as described elsewhere (25). After removal of the excess of the reagent on a small NAP-10 column (Pharmacia, Uppsala, Sweden), the only reactive thiol in the absence of nucleotide is Cys-177 on light chain A1; this residue was modified with 1,5-IAEDANS (Molecular Probes or Sigma) using a 7-fold molar excess of the reagent for 5 h. The reaction was stopped, and the protective dinitrobenzene group was removed from SH1 by adding ~50 mM DTE (Serva, Heidelberg, Germany) and leaving the protein overnight on ice. The excess of the dye and DTE was removed on a small Sephadex G-25 column equilibrated with buffer F₂₀, consisting of 20 mM MOPS, pH 7.5, 20 mM NaCl, 2 mM MgCl₂, and 0.2 mM DTE. The

labeling stoichiometry was 0.98 ± 0.10 . Since the protection of Cys-707 by 2,4-dinitro-1-fluorobenzene is incomplete, we used two methods to assess the amount of residual label on SH1. More than 85% of K⁺/EDTA ATPase was recovered after the thiolysis by DTE as described above. This result was in full agreement with the SDS–PAGE electrophoresis of S1 and its fragments produced by limited trypsinolysis. As shown previously (25), no more than 15% of 1,5-IAEDANS fluorescence was associated with the heavy chain of S1, and this label was found exclusively in the 20 kDa terminal fragment. The rest of the dye was located on the essential light chain A1. Trinitrophenylation of Lys-83 was done as described by Mornet et al. (26). The reaction of 2,4,6-trinitrobenzenesulfonic acid (TNBS) with S1 is biphasic: the rapid phase, corresponding to the modification of Lys-83, is followed by a much slower modification of other lysyl residues (27). A 10-fold molar excess of TNBS (Sigma) was used, and the reaction was arrested at the onset of the second phase by lowering the pH to 6.5 with concentrated imidazole and passing the protein through a G-25 column to remove unreacted TNBS. This method produced a protein with a dye/protein ratio slightly greater than 1. The labeling of Lys-553 with FHS (Fluka) was performed as described recently (28), yielding a product containing 0.95 ± 0.25 mol of FHS/mol of S1. Protein concentration was estimated either from absorption, subtracting the contribution of the dye at 280 nm, or by using the Bradford assay. The following extinction coefficients were used: S1, $\epsilon_{280}^{1\%} = 7.5$; 1,5-IAEDANS, $6.1 \text{ mM}^{-1} \text{ cm}^{-1}$ at 337 nm; TNP-S1, $14.5 \text{ mM}^{-1} \text{ cm}^{-1}$ at 345 nm; TNP-ADP, $26.4 \text{ mM}^{-1} \text{ cm}^{-1}$ at 408 nm; FHS-S1, $68 \text{ mM}^{-1} \text{ cm}^{-1}$ at 495 nm.

Preparation of Transition State Complexes of S1 with BeF_x, AlF₄[−], and VO₄^{3−}. These complexes were prepared by the method of Werber et al. (19). Briefly, the solution of S1 in buffer F₂₀ was incubated for 5 min with 0.2 mM ADP and, for BeF_x and AlF₄[−], with 5 mM NaF (Merck). Next, BeSO₄, AlCl₃ (both from Merck), or VO₄^{3−} (Aldrich) was added to a final concentration of 0.2 mM and the incubation continued for 15 min. A stock solution of vanadate was prepared according to Goodno (29) and kept

at pH 10; just before the experiments an aliquot of the stock solution was neutralized with 0.5 M MOPS, pH 7, and used for measurements. For FRET experiments, the transition state complexes were usually prepared directly in the cuvette using a protein concentration of 1–2 μ M. The solutions were exposed to the excitation beam only for the time necessary to perform the measurements. Since all of the analogs bind to the active site of S1 producing inactive complexes, the degree of incorporation into S1 was estimated from the enzymatic activity. For the 1,5-IAEDANS–S1, the K^+ /EDTA activity was 89%, 93%, and 98% inhibited in the presence of BeF_x , AlF_4^- , and vanadate, respectively. For 1,5-IAEDANS–TNP-ADP·S1A1, these numbers were 82%, 87%, and 95%; for 1,5-IAEDANS–FHS-S1A1, the degree of inhibition was 97%, 82%, and 99%. For 1,5-IAEDANS–TNP-S1A1 (label on Lys-83), the Mg^{2+} -ATPase rather than its K^+ /EDTA activity was measured, and the degrees of inhibition were 91%, 88%, and 68% for the complexes with BeF_x , AlF_4^- , and VO_4^{3-} , respectively. Thus the formation of the transition state complexes occurred efficiently also for the modified protein.

Steady-state fluorescence spectroscopy was used to measure the degree of quenching of the donor fluorescence, *viz.*, the efficiency of energy transfer. Three factors which may distort the real value of the transfer were taken into account. (1) The exact concentration (and therefore the fluorescence intensity) of the donor is difficult to measure especially for doubly labeled proteins. (2) There may occur inner filter effects (reabsorption), particularly for strongly absorbing acceptors, e.g., FHS. (3) The acceptor may contribute to the total emission at the donor wavelength. In order to eliminate the first factor, we compared fluorescence of the labeled proteins in the presence of 1% SDS. While SDS may not induce the random-coil conformation of S1, it dissociates the light chain from the heavy chain, eliminating all energy transfer, enabling us to normalize the donor concentration. Factors 2 and 3 can be eliminated by the use of appropriate emission and excitation wavelengths. We found that, with excitation at 340 nm and emission at 465 nm, contributions from factors 2 and 3 were negligible, except when TNP-ADP was used as an acceptor; in this case, we excited the fluorescence at 360 nm and analyzed the emission at 510 nm. We also used quartz semi-microcuvettes (0.4×1 cm, Hellma, Germany) to further attenuate the inner filter effect. When TNP-ADP was employed as an acceptor, the amount of nonspecifically bound nucleotide was estimated with the use of ADP as described elsewhere (30). All fluorescence measurements were performed using a Kontron SFM-25 fluorometer, interfaced to a microcomputer, at room temperature in buffer F₂₀. The spectra were smoothed using a published algorithm (31).

The quantum yield of 1,5-IAEDANS conjugated with Cys-177 on light chain A1 was taken as 0.40 (30). If the value of 0.3 is used instead (30), the values of R_0 in Table 1 and the corresponding distances have to be reduced by about 4.5%. Details are given in the legend to Table 1. All values in Table 1 were corrected for the presence of 15% of the donor on Cys-707. This was done by using published values of FRET efficiencies (E) or obtaining these values experimentally. For the Cys-707 \rightarrow Lys-83, $E = 0.70$ (33); for the Cys-707 \rightarrow TNP-ADP, $E = 0.56$ (34). The efficiency of transfer between Cys-707 and Lys-553 was measured in a separate experiment (data not shown), and a value of E

Table 1: Distances between 1,5-IAEDANS Conjugated with Cys-177 (Alkali Light Chain 1) and Chromophores Bound to Lys-83, the Active Site, and Lys-553

| complex | FRET efficiency | distance (Å) | change in distance (Å) |
|--|-----------------|--------------|------------------------|
| Cys-177 (A1) \rightarrow Lys-83 ^a | | | |
| S1 | 0.442 | 25.2 | |
| S1·MgADP ^b | 0.449 | 25.1 | −0.1 |
| S1 + MgATP ^b | 0.427 | 25.5 | 0.3 |
| S1·MgADP·BeF _x | 0.410 | 25.8 | 0.6 |
| S1·MgADP·AlF ₄ | 0.389 | 26.2 | 1.0 |
| S1·MgADP·VO ₄ | 0.384 | 26.3 | 1.1 |
| acto-S1 ^c | 0.430 | 25.4 | 0.2 |
| acto-S1 + MgADP ^{b,c} | 0.410 | 25.8 | 0.6 |
| Cys-177 (A1) \rightarrow TNP-ADP (active site) ^d | | | |
| S1·MgTNP-ADP | 0.112 | 55.3 | |
| S1·MgTNP-ADP·BeF _x | 0.215 | 48.9 | −6.4 |
| S1·MgTNP-ADP·AlF ₄ | 0.198 | 49.5 | −5.8 |
| S1·MgTNP-ADP·VO ₄ | 0.137 | 53.4 | −1.9 |
| Cys-177 (A1) \rightarrow Lys-553 (actin binding site) ^e | | | |
| S1 | 0.342 | 50.6 | |
| S1·MgADP ^b | 0.335 | 50.9 | 0.3 |
| S1 + MgATP ^b | 0.278 | 53.2 | 2.6 |
| S1·MgADP·BeF _x | 0.356 | 50.1 | −0.5 |
| S1·MgADP·AlF ₄ | 0.386 | 49.0 | −1.5 |
| S1·MgADP·VO ₄ | 0.306 | 52.0 | 1.4 |
| acto-S1 ^c | 0.421 | 47.8 | −2.8 |
| acto-S1 + MgADP ^{b,c} | 0.357 | 50.1 | −0.5 |

^a The values of transfer efficiency were obtained from donor quenching data ($\lambda_{\text{ex}} = 340$ nm; $\lambda_{\text{em}} = 465$ nm). The distances shown correspond to the quantum yield of the donor (q_D) equal to 0.40 (30), $J = 3.36 \times 10^{13} \text{ M}^{-1} \text{ nm}^4 \text{ cm}^{-1}$, and $R_0 = 24.3$ Å. For $q_D = 0.30$ (32), $R_0 = 23.1$ Å, and all distances for this donor–acceptor pair have to be reduced by 4.4%. ^b 1 mM ADP or 1 mM ATP. ^c F-Actin was supplemented with an equimolar amount of phalloidin (Sigma) and used at 3-fold molar excess over S1. ^d To correct for nonspecific binding of TNP-ADP to S1, the values of transfer efficiency (E) were calculated from the following equation: $E = -(F_{\text{TNP-ADP}} - F_{\text{ADP}})/F_{\text{ADP}}$, where $F_{\text{TNP-ADP}}$ and F_{ADP} denote the value of the donor fluorescence intensity at 510 nm and excitation at 360 nm (to minimize the inner filter effect of TNP-ADP) in the presence of 6 μ M TNP-ADP and upon subsequent addition of 1 mM ADP, respectively. The contributions from nonspecific binding of TNP-ADP to the values of E in complexes of TNP-ADP with BeF_x , AlF_4 , and vanadate were corrected for by preparing these complexes and measuring changes in the fluorescence intensity of the donor in the presence of 6 μ M TNP-ADP and 1 mM ADP. The value of $K_d(\text{TNP-ADP})$ is 0.3 μ M (30). The distances shown correspond to the quantum yield of the donor equal to 0.40 (30), $J = 5.94 \times 10^{14} \text{ M}^{-1} \text{ nm}^4 \text{ cm}^{-1}$, and $R_0 = 39.2$ Å. For $q_D = 0.30$ (32), $R_0 = 37.4$ Å, and all distances for this donor–acceptor pair have to be reduced by 4.7%. ^e The values of transfer efficiency were obtained from donor quenching data at $\lambda_{\text{ex}} = 340$ nm and $\lambda_{\text{em}} = 465$ nm. The distances shown correspond to the quantum yield of the donor equal to 0.40 (30), $J = 1.45 \times 10^{15} \text{ M}^{-1} \text{ nm}^4 \text{ cm}^{-1}$, and $R_0 = 45.4$ Å. For $q_D = 0.30$ (32), $R_0 = 43.3$ Å, and all distances for this donor–acceptor pair have to be reduced by 4.5%.

equal to 0.37 was obtained. The corrected values of the transfer (E_{corr}) were computed using the equation $E_{\text{corr}} = (E_{\text{measured}} - 0.15E_{707})/0.85$, where E_{707} denotes the transfer efficiency from Cys-707 to Lys-83, TNP-ADP, or Lys-553. All these corrections were generally small and did not affect any of the conclusions reached in this paper. The values of the overlap integrals in the Förster equation were obtained by numerical integration. The orientation factor κ^2 of $2/3$ and the refractive index of 1.4 were assumed for the three donor–acceptor pairs. No Dale–Eisinger analysis was performed since two of the acceptors used are nonfluorescent. It is noteworthy, however, that the donor possesses a

considerable degree of rotational freedom (30), and the polarization of FHS-S1 is low (A. A. Kasprzak and C. Smyczynski, unpublished observation); hence the assumption $\kappa^2 = 2/3$ is unlikely to yield seriously inaccurate distances. The equations used to compute the R_0 values and the interchromophore distances were the same as in ref 35. Values of all FRET parameters are given in footnotes to Table 1.

Proteolytic digestion of S1 by trypsin was done in 20 mM MOPS, pH 8, using a ratio of 1:20 w/w trypsin:S1 for 20 min at room temperature. When the effects of nucleotides and nucleotide analogs on the S1 digestion were examined, the buffer contained also Mg^{2+} (2 mM), nucleotide, and $BeSO_4$, $AlCl_3$, or V_i at a concentration of 0.2 mM and, in the case of beryllium and aluminum, 5 mM NaF. Digestion of S1 by endoproteinase Arg-C (Boehringer Mannheim, Germany) was performed in 30 mM MOPS and 0.1 mM NaN_3 , pH 8, employing 15 units of Arg-C/mg of 1,5-IAEDANS-S1A1 for 2.5 h at 25 °C.

Cross-linking of Cys-697 (SH2) to the 50 kDa fragment of S1 was done with pPDM for 1.5 h at 4 °C, using Arg-C-cut 1,5-IAEDANS-S1A1 (3.5 mg/mL). The digested and/or cross-linked products were analyzed by SDS-PAGE.

The ATPase activity of S1 was measured by a colorimetric assay in a buffer containing 50 mM tris(hydroxymethyl)-aminomethane, pH 8.0, and either 1 M KCl supplemented with 5 mM EDTA or 2.5 mM $MgCl_2$ and 10 mM KCl. The reaction was initiated by the addition of ATP (2 mM) and was stopped with 15% trichloroacetic acid. The concentration of the phosphomolybdate complex formed was measured from its absorption at 660 nm, using the procedure of Lopez and Lowry, as described in ref 36.

RESULTS

How Much Change in FRET Is Expected? We have computed the anticipated changes in the distances from Cys-177 to Lys-83, the active site [represented by Asn-127 which forms a hydrogen bond with the ATP ribose oxygen O4' (20)], and Lys-553 when the putative lever arm rotates by the given angle (Figure 2A–C). Two pivot points (both conserved glycine residues) were employed in these calculations: Gly-699 (9, 10) and Gly-770 (6). The initial value of the transfer efficiency, i.e., E for no rotation, was either the experimentally measured FRET (see below) or the efficiency based on the distance obtained from the x-ray structure. Both types of curves are shown in Figure 2D–F. They have similar shapes, indicating that the discrepancies between the FRET and X-ray-derived distances do not have a significant impact on the magnitude of the expected changes in FRET that result from the rotation of the α -helix.

Since the acceptors were attached to points located rather far from either of the fulcrums, it is not surprising that the expected changes are substantial, particularly for the Cys-177 \rightarrow Lys-83 distance (Figure 2A,D). For the distance to the active site, the magnitude and the direction of change (increase or decrease in FRET) depend on the choice of the pivot point (Figure 2B,E). With the lever rotating as a rigid body around Gly-770, a decrease in FRET (increase in the distance) is expected, whereas rotations around Gly-699 should result in an increase in FRET. The third distance, Cys-177 \rightarrow Lys-553, is rather long, and only a small change in FRET should be seen for small angles of rotation ($\leq 20^\circ$)

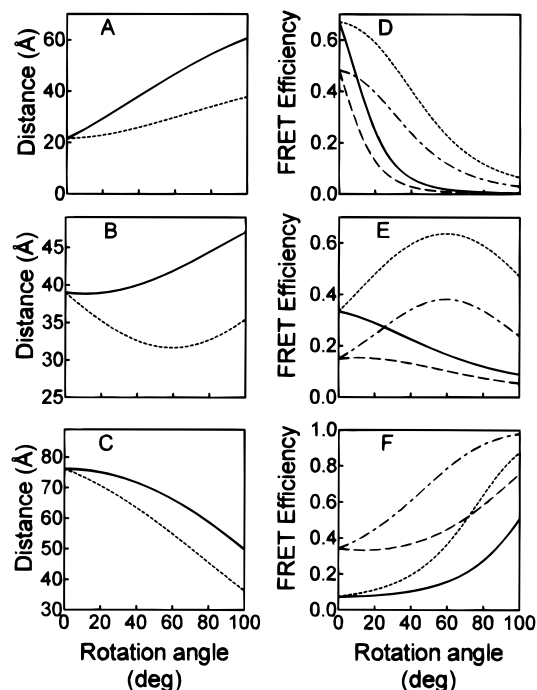


FIGURE 2: Expected alterations of the interprobe distances (left) and the corresponding changes in FRET (right) resulting from rotation of the putative lever arm of S1. The light chain-binding domain of S1 was rotated in the plane of the actin filament, similarly to the movement seen in smooth muscle S1 on addition of ADP (ref 6 and R. Milligan, personal communication). Two hypothetical pivot points were used: (—, — —) Gly-699 and (---, - · -) Gly-770. Panels (A, D) Cys-177 \rightarrow Lys-83; (B, E) Cys-177 \rightarrow active site; (C, F) Cys-177 \rightarrow Lys-553. The efficiency of FRET was either computed from the X-ray structure (curves — and ---) or measured experimentally (FRET in the absence of nucleotides) (curves - · - and - · -). The coordinates of the acto-S1 complex (54) were provided by I. Rayment and used with his permission.

(Figure 2C,F). However, as shown in Figure 2, a dramatic change in FRET is expected for large angles of rotation ($\geq 50^\circ$).

Could the Modifications of the Functional Groups of S1 Have Rendered It Incapable of Moving Its Lever Arm? Modification of Cys-177 on the essential light chain is not known to change any enzymatic or actin-binding characteristics of S1. Likewise, conjugation of labels to Lys-553 also did not have a major effect on either its enzymatic activity or actin binding (28). However, trinitrophenylation of myosin leads to marked changes in its ATPase activity (27). Therefore, we performed several experiments to assess the effect of Lys-83 on the intersite communication in S1.

We measured the degree of nucleotide trapping by beryllium, aluminum, and V_i (see Experimental Procedures). These results indicate that TNP-S1 was fully competent of forming the complexes with these ligands. We studied the effect of nucleotides and nucleotide analogs on the digestion pattern of S1 by trypsin. The presence of nucleotides has a pronounced effect on the cleavage pattern of S1 by trypsin and several other proteases (37). When trypsin is used with native S1, two of the three proteolytic fragments initially produced are partially degraded. Both the 50 and the 27 kDa fragments are digested to yield two new fragments with a molecular mass of 22 and 45 kDa, respectively. Such a digestion pattern was seen for native S1 and also for TNP-S1 (data not shown). Furthermore, in the presence of the transition state analogs, the 27 kDa fragment completely

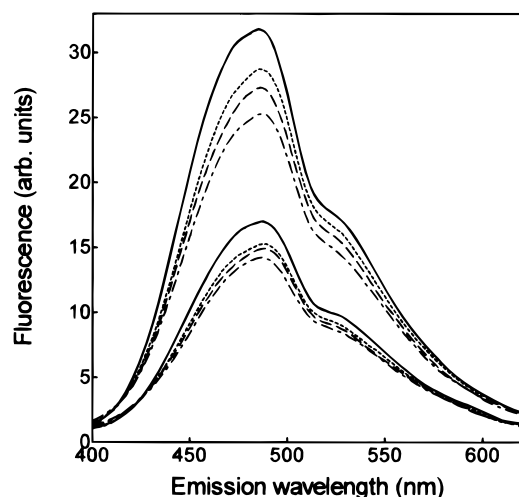


FIGURE 3: Effects of ADP and ADP·BeF_x on the fluorescence resonance energy transfer between Cys-177 (light chain A1) and Lys-83 (heavy chain). The top set of curves was obtained for S1 labeled only with the donor (1,5-IAEDANS); the bottom curves were obtained for the donor in the presence of the acceptor (TNBS). (—) S1A1, 1 μ M; (---) S1A1 + ADP, 0.2 mM; (—) S1A1 + ADP + NaF, 5 mM, incubated for 5 min; (---) same as (—) but after 15 min incubation with 0.2 mM BeSO₄.

disappeared for both the native and the trinitrophenylated S1 (data not shown). This indicates that the communication between the active site and surface loops 1 and 2 was not impaired by the trinitrophenylation. Other findings are in agreement with this notion. It was reported that digestion patterns of S1 by thermolysin and subtilisin were unaffected by modification of Lys-83 (38). The same authors also showed that trinitrophenylation of this residue neither changed the susceptibility of S1 to thermal inactivation nor affected the V_i-dependent photocleavage of S1 (38). Finally, it was demonstrated that the effect of binding of nucleotides to the active site of S1 is transmitted along the α -helix to Cys-177 of the light chain, since fluorescence intensity of labels conjugated to this residue is influenced by these ligands (32). In Figure 3, we show that this effect also persists for TNP-S1, and furthermore, it is intensified by the metallofluorides and V_i. Although some other properties of TNP-S1 are noticeably altered by the modification (27, 38), these changes appear to be restricted to the nucleotide binding site of the protein.

We also performed a series of experiments to examine conformational changes induced by TNP-ADP in S1. We found that TNP-ATP is a good substrate for the S1 ATPase: the K⁺/EDTA activity was $104 \pm 12\%$, and the Ca²⁺ activity was $161 \pm 37\%$ of the corresponding values for ATP. In the presence of TNP-ADP, stable complexes with beryllium, aluminum, and V_i were formed (see Experimental Procedures). In order to check if TNP-nucleotides were able to trigger structural changes in the myosin head similar to unmodified nucleotides, we examined the effect of TNP-nucleotides on the proteolysis of S1 by trypsin. Both TNP-ADP and TNP-ATP were effective in promoting a partial degradation of the 27 and 50 kDa fragments in a fashion very similar to that of ADP and ATP (data not shown). Furthermore, formation of the complexes with beryllium, aluminum, and V_i facilitated this conversion. We also tested the ability of TNP-ADP to promote a covalent cross-linking of Cys-697 (SH2) to the 50 kDa fragment by pPDM (39) in S1 for which the 50–20 kDa loop was cleaved by endopro-

teinase Arg-C. Again, similarly to ADP, TNP-ADP alone and in complexes with metallofluorides and V_i was effective in supporting the production of such covalent union (data not shown). Finally, it is noteworthy that both the 2'- and the 3'-hydroxyls of the ADP ribose are exposed to the solvent. This explains the fact that the presence of an additional group in this position, such as in TNP-ADP, was found to be well tolerated by myosin (40, 41).

In sum, there exist many lines of experimental evidence supporting the view that the modification of Lys-83 or the substitution of TNP-ADP for ADP will not impair the ability of S1 to undergo the structural alterations in the presence of Be, Al, and V_i. However, one has to bear in mind that all the evidence presented above is indirect; hence, there is no direct proof that the modified proteins in the presence of the nucleotide analogs produce a conformational state of the head that closely resembles the structure of S1·ADP·P_i.

The Interprobe Distances in the Absence of Nucleotides. For Cys-177 \rightarrow Lys-83 the crystallographically derived distance is 21.6 Å, and the measured separation of the probe is 25.2 Å (Table 1). The exact position of the trinitrophenyl ring conjugated with the ribose of active site-bound TNP-ADP is not known. However, we can fix the limits of the Cys-177 \rightarrow active site distance from the position of adjacent amino acid residues or ions. From the X-ray structure we calculated that the lower limit corresponding to the Cys-177 \rightarrow Asn-127 distance is 40 Å and the upper limit taken as the separation between Cys-177 \rightarrow SO₄²⁻ is 48 Å. The FRET-measured distance is 55.3 Å, which is somewhat too long compared to the X-ray structure but in good agreement with the published value of 57 Å (30). The value of the third distance Cys-177 \rightarrow Lys-553 is 50.6 Å when measured by FRET and *ca.* 76 Å from X-ray crystallography. However, the uncertainty regarding its *absolute value* is large in this case: the label not only possesses a long linker but also is attached to a rather long side chain (lysine).

The Effect of Nucleotides, Phosphate Analogs, and Actin on the Distances. For the Cys-177 \rightarrow Lys-83 distance, no changes were seen in the presence of ATP, ADP, metallofluorides, vanadate, and actin in the presence and absence of ADP (Table 1, Figure 3). The standard error for these measurements is about 1.2 Å.

The distance from Cys-177 to the active site decreased in the presence of the phosphate analogs (Table 1). For beryllium complexes the standard error was 3.6 Å; for aluminum and vanadate, about 2 Å. The changes for MgADP·BeF_x and MgADP·AlF₄⁻ correspond to rotations of $\sim 35^\circ$ but only if the fulcrum point is located at Gly-770 (Figure 2). For MgADP·VO₄³⁻, the angular reorientation is quite small ($<15^\circ$). We do not believe that the changes in the FRET efficiency observed for complexes with BeF_x and AlF₄⁻ correspond to reorientation of the light chain-binding domain of S1. First, the change is most pronounced for the beryllium complex and very small (within experimental error) for the vanadium complex. Exactly opposite behavior is expected from the X-ray structures of these complexes (8, 20). Second, in order to see a decrease in the Cys-177 \rightarrow active site distance, the pivot point must reside at Gly-770; pivoting around Gly-699 leads to an augmentation of the distance (Figure 2). There are several lines of evidence that the fulcrum is located inside the catalytic domain of S1, probably near or at the Cys-697–Cys-707 helix (9, 10, 42) rather than at Gly-770. Third, a

rotation of that magnitude should be easily detected by the other two probes, but no such changes were seen. Two explanations can be offered for the observed effect of BeF_x and AlF_4^- on the separation $\text{Cys-177} \rightarrow$ active site: the trinitrophenyl ring of TNP-ADP altered its orientation in the presence of BeF_x and AlF_4^- . This chromophoric part of the nucleotide is exposed and has some freedom to move (40). Another possibility is that TNP-ADP has a secondary binding site on myosin that can interfere with the present FRET measurements.

Nucleotides and actin have little influence on the third distance ($\text{Cys-177} \rightarrow \text{Lys-553}$) (Table 1). These changes were within the experimental error, which was ± 2.5 Å; this translates into a rotation of about 25° .

DISCUSSION

Can These Findings Be Reconciled with the Lever Arm Hypothesis? The presence of two structural domains in S1, correctly deduced from birefringence measurements (43), leads naturally to a model in which a portion of the protein changes its orientation (44). Subsequently, changes in hydrodynamic parameters of S1 on addition of nucleotides were confirmed in a number of laboratories (14, 45–48). But only recently the results obtained by several independent methods converged on the rotating lever arm hypothesis. The data in this paper seem, on the surface, to contradict the basic tenet of this hypothesis. We note that our results do not contradict the hydrodynamic data because the reorientation of the helix was found to be in the order of 30° or less (46, 47), what is consistent with the present experiments (see Results). One can argue that the reorientation of the lever occurs only when the myosin head is bound to actin. Such a hypothesis must be rejected: in the presence of actin, the distances—and implicitly, the lever orientation—are the same as in the $\text{ADP}\cdot\text{P}_i$ state: any changes produced only when the head is bound to actin would have to be reversed, producing no effective work. Below we offer three plausible models of force generation by S1. In all of them the light chain-binding domain may act as a lever: however, $\text{ADP}\cdot\text{P}_i$ or the metallofluoride complexes would not produce major changes in the distances measured in this work.

(1) In the $\text{S1}\cdot\text{ADP}\cdot\text{P}_i$ state, the light chain-binding domain bends uniformly along its length rather than rotating as a rigid body. In such a case, points located in the middle of the helix (such as residues of the essential light chain) would move by relatively small distances that may be difficult to detect. Theoretical calculations (49) support the idea that bending of the light chain-binding domain of S1 could provide enough elasticity to store the energy of ATP hydrolysis. Also, recent observations indicate that the distance between the regulatory and the essential light chains changes when nucleotides are added to S1 (P. Fajer and B. Hambly, personal communication).

(2) There exist two conformers of $\text{S1}\cdot\text{ADP}\cdot\text{P}_i$ in thermodynamic equilibrium; however, the fraction containing the lever arm in the “beginning-of-the-power-stroke” state is small, and therefore it could not be detected by the present FRET measurements. The presence of two S1 conformations was proposed for first time in 1981 (50). This idea was found to be consistent with many results obtained by the Cheung group (45, 51).

(3) Finally, one can also suggest that, in the presence of nucleotides, the long α -helical segment adopts an entire

spectrum of orientations relative to the heavy chain, but FRET, when measured in a steady-state experiment, cannot reveal the underlying distance distribution. Binding to actin traps a prestrained cross-bridge, so the system operates as a some sort of Brownian ratchet (52). This mechanism agrees well with the behavior of certain spectroscopic probes attached to the regulatory light chain of scallop S1 (53).

In conclusion, the measured changes in the distances between the light chain binding and the catalytic domain of S1 seem too small to be in agreement with a simple two-position lever arm model. The reorientation of the light-binding domain during force generation appears to be small ($\leq 25^\circ$) or the coupling of the ATP hydrolysis to the movement of the head may involve one of the mechanisms described briefly above. It is important to note that these alternative mechanisms proposed above can be tested experimentally. For example, the presence of multiple orientations of the putative lever arm should manifest itself as a distance distribution in time-resolved FRET measurements. Such experiments are indeed in progress.

ACKNOWLEDGMENT

We are indebted to Ivan Rayment for providing the coordinates of the acto-S1 complex. We thank Patrick Chaussepied for critically reading the paper, helpful suggestions and illuminating discussions and Ridha Kassab for continuing interest in this work.

REFERENCES

1. Rayment, I., Rypniewski, W. R., Schmidt-Bäse, K., Smith, R., Tomchick, D. R., Benning, M. M., Winkelman, D. A., Wesenberg, G., and Holden, H. M. (1993) *Science* 261, 50–58.
2. Molloy, J. E., Burns, J. E., Kendrick-Jones, J., Tregear, R. T., and White, D. C. S. (1995) *Nature* 378, 209–212.
3. Finer, J. T., Simmons, R. M., and Spudich, J. A. (1994) *Nature* 368, 113–119.
4. Guilford, W. H., Dupuis, D. E., Kennedy, G., Wu, J., Patlak, J. B., and Warshaw, D. M. (1997) *Biophys. J.* 72, 1006–1021.
5. Holmes, K. C. (1997) *Curr. Biol.*, 7, R112–R118.
6. Whittaker, M., Wilson-Kubalek, E. M., Smith, J. E., Faust, L., Milligan, R. A., and Sweeney, H. L. (1995) *Nature* 378, 748–751.
7. Jontes, J. D., Wilson-Kubalek, E. M., and Milligan, R. A. (1995) *Nature* 378, 751–753.
8. Smith, C. A., and Rayment, I. (1996) *Biochemistry* 35, 5404–5417.
9. Uyeda, T. Q., Abramson, P. D., and Spudich, J. A. (1996) *Proc. Natl. Acad. Sci. U.S.A.* 93, 4459–4464.
10. Kinose, F., Wang, S. X., Kidambi, U. S., Moncman, C. L., and Winkelman, D. (1996) *J. Cell Biol.* 134, 895–909.
11. Gollub, J., Cremo, C., and Cooke, R. (1996) *Nat. Struct. Biol.* 3, 796–801.
12. Anson, M., Geeves, M. A., Kurzawa, S. E., and Manstein, D. J. (1996) *EMBO J.* 15, 6069–6974.
13. Waller, G. S., Ouyang, G., Swafford, J., Vibert, P., and Lowey, S. (1995) *J. Biol. Chem.* 270, 15348–15352.
14. Wakabayashi, K., Tokunaga, M., Kohno, I., Sugimoto, Y., Hamanaka, T., Takezawa, Y., Wakabayashi, T., and Amemiya, Y. (1992) *Science* 258, 443–447.
15. Allen, T. St. C., Ling, N., Irving, M., and Goldman, Y. (1996) *Biophys. J.* 70, 1847–1862.
16. Block, S. (1996) *Cell* 87, 151–157.
17. Barsotti, R. J., Dantzig, J. A., and Goldman, Y. E. (1996) *Nat. Struct. Biol.* 3, 737–739.
18. Howard, J. (1996) *Annu. Rev. Physiol.* 58, 703–729.
19. Werber, M. M., Peyser, Y. M., and Muhrad, A. (1992) *Biochemistry* 31, 7190–7197.

20. Fisher, A. J., Smith, C. A., Thoden, J. B., Smith, R., Sutoh, K., Holden, H. M., and Rayment, I. (1995) *Biochemistry* 34, 8960–8972.
21. Phan, B. C., Peyser, Y. M., Reisler, E., and Muhlrads, A. (1997) *Eur. J. Biochem.* 243, 636–642.
22. Smoczynski, C., and Kasprzak, A. A. (1997) *Biophys. J.* 72, A18.
23. Kasprzak, A. A. (1993) *J. Biol. Chem.* 268, 13261–13266.
24. Zaager, S., and Burke, M. (1988) *J. Biol. Chem.* 263, 1513–1517.
25. Kasprzak, A. A., Chaussepied, P., and Morales, M. F. (1989) *Biochemistry* 28, 9230–9238.
26. Mornet, D., Pantel, P., Bertrand, R., Audemard, E., and Kassab, R. (1980) *FEBS Lett.* 117, 183–188.
27. Muhlrads, A., Lamed, R., and Oplatka, A. (1975) *J. Biol. Chem.* 250, 175–181.
28. Bertrand, R., Derancourt, J., and Kassab, R. (1995) *Biochemistry* 34, 9500–9507.
29. Goodno, C. C. (1982) *Methods Enzymol.* 85, 116–123.
30. Moss, D., and Trentham, D. R. (1983) *Biochemistry* 22, 5261–5270.
31. Gorry, P. A. (1990) *Anal. Chem.* 62, 570–573.
32. Marsh, D. J., and Lowey, S. (1980) *Biochemistry* 19, 774–784.
33. Takashi, R., Muhlrads, A., and Botts, J. (1982) *Biochemistry* 21, 5661–5668.
34. Tao, T., and Lamkin, M. (1981) *Biochemistry* 20, 5051–5055.
35. Takashi, R., and Kasprzak, A. A. (1987) *Biochemistry* 26, 7471–7477.
36. Leloir, L. F., and Cardini, C. E. (1957) *Methods Enzymol.*, 3, 840–850.
37. Mornet, D., Pantel, P., Audemard, E., Derancourt, J., and Kassab, R. (1985) *J. Mol. Biol.* 183, 479–489.
38. Phan, B. C., Cheung, P., Miller, C. J., Reisler, E., and Muhlrads, A. (1994) *Biochemistry* 33, 11286–11295.
39. Chaussepied, P., Mornet, D., and Kassab, R. (1986) *Proc. Natl. Acad. Sci. U.S.A.* 83, 2037–2041.
40. Cremona, C., Neuron, J., and Yount, R. G. (1990) *Biochemistry* 29, 3309–3319.
41. Crowder, M. S., and Cooke, R. (1987) *Biophys. J.* 51, 323–333.
42. Guilford, W. H., Lauzon, A. M., Freyzon, Y., Warshaw, D. M., and Trybus, K. M. (1997b) *Biophys. J.* 72, A221.
43. Highsmith, S., and Eden, D. (1986) *Biochemistry* 25, 2237–2242.
44. Cooke, R. (1986) *CRC Rev. Biochem.* 21, 53–118.
45. Aguirre, R., Lin, S. H., Gonsoulin, F., Wang, C. K., and Cheung, H. C. (1989) *Biochemistry* 28, 799–807.
46. Highsmith, S., and Eden, D. (1990) *Biochemistry* 29, 4087–4093.
47. Sugimoto, Y., Tokunaga, M., Takezawa, Y., Ikebe, M., and Wakabayashi, K. (1995) *Biophys. J.* 68, 29s–34s.
48. Mendelson, R. A., Schneider, D. K., and Stone, D. B. (1996) *J. Mol. Biol.* 256, 1–7.
49. Howard, J., and Spudich, J. A. (1996) *Proc. Natl. Acad. Sci. U.S.A.* 93, 4462–4464 (Appendix to ref 9).
50. Shriver, J. W., and Sykes, B. D. (1981) *Biochemistry* 20, 2004–2012.
51. Lin, S. H., and Cheung, H. C. (1991) *Biochemistry* 30, 4317–4322.
52. Peskin, C. S., Odell, G., and Oster, G. F. (1993) *Biophys. J.* 65, 316–324.
53. Thomas, D. D., Ramachandran, S., Roopnarine, O., Hayden, D. W., and Ostap, E. M. (1995) *Biophys. J.* 68, 135s–141s.
54. Rayment, I., Holden, H. M., Whittaker, M., Yohn, C. B., Lorenz, M., Holmes, K. C., and Milligan, R. A. (1993) *Science* 261, 58–65.

BI9707461